THE JOURNAL OF COMPARATIVE NEUROLOGY 481:363–376 (2005)

Medial Prefrontal Cortex Control of the Paraventricular Hypothalamic Nucleus Response to Psychological Stress: Possible Role of the Bed Nucleus of the Stria Terminalis

SARAH J. SPENCER,* KATHRYN M. BULLER, AND TREVOR A. DAY
School of Biomedical Sciences, Department of Physiology and Pharmacology, University of Queensland, Brisbane QLD 4072, Australia

ABSTRACT

The medial prefrontal cortex (mPFC) has been strongly implicated in control of the paraventricular nucleus of the hypothalamus (PVN) response to stress. Because of the paucity of direct projections from the mPFC to the PVN, we sought to investigate possible brain regions that might act as a relay between the two during psychological stress. Bilateral ibotenic acid lesions of the rat mPFC enhanced the number of Fos-immunoreactive cells seen in the PVN after exposure to the psychological stressor, air puff. Altered neuronal recruitment was seen in only one of the candidate relay populations examined, the ventral bed nucleus of the stria terminalis (vBNST). Furthermore, bilateral ibotenic acid lesions of the BNST caused a significant attenuation of the PVN response to air puff. To better characterize the structural relationships between the mPFC and PVN, retrograde tracing studies were conducted examining Fos expression in cells retrogradely labeled with cholera toxin b subunit (CTb) from the PVN and the BNST. Results obtained were consistent with an important role for both the mPFC and BNST in the mpPVN CRF cell response to air puff. We suggest a set of connections whereby a direct PVN projection from the ipsilateral vBNST is involved in the mpPVN response to air puff and this may, in turn, be modulated by an indirect projection from the mPFC to the BNST. J. Comp. Neurol. 481:363–376, 2005.

Indexing terms: Fos; ibotenic acid; cholera toxin b subunit; air puff

The paraventricular nucleus of the hypothalamus (PVN) is known to play a major role in generating adaptive autonomic, behavioral, and hormonal responses to stress (Sawchenko et al., 1996; Herman and Cullinan, 1997). Many previous investigations have focused on the identity of inputs to the PVN that might drive these responses. However, given the desire to eventually develop new approaches to suppressing overactive stress responses, an important alternative is to consider inputs that might suppress and thus limit the activation of the PVN with stress.

One brain region that has been suggested to suppress key components of the body's stress response, including PVN responses to psychological stress, is the medial prefrontal cortex (mPFC). A variety of autonomic, behavioral, and endocrine responses to stress are potentially inhibited by activation of the mPFC. For example, mPFC activation generates cardiovascular depressor responses and has an inhibitory influence on sympathetic vasomotor function (Verberne and Owens, 1998). The mPFC also acts to suppress various behavioral responses to stress (Espejo and Minano, 1999; Lacroix et al., 2000), and the region is involved in suppression of endocrine responses to some stressors (Diorio et al., 1993; Brake et al., 2000; van Eden and Buijs, 2000; Crane et al., 2003b). Given the pivotal role of the PVN in the shaping of integrated stress re-

Grant sponsor: National Health and Medical Research Council of Australia; Grant number: NHMRC 110362.

*Correspondence to: Sarah J. Spencer, School of Biomedical Sciences, Department of Physiology and Pharmacology, University of Queensland, Brisbane QLD 4072, Australia. E-mail: spences@ucalgary.ca

Received 30 January 2004; Revised 29 June 2004; Accepted 1 September 2004

DOI 10.1002/cne.20376

Published online in Wiley InterScience (www.interscience.wiley.com).

sponses, it is not surprising to find that mPFC suppression of stress responses also involves a modulation of PVN output (Figueiredo et al., 2003). However, important questions remain unanswered concerning the identity of the brain pathways involved.

Importantly, anatomical studies have failed to demonstrate direct projections from the mPFC to the PVN (Hurley et al., 1991; Floyd et al., 2001). Accordingly, the mechanism by which the mPFC modulates PVN stress responses is likely to involve a relay or relays through other brain regions. Candidate relay populations include the medial regions of the hypothalamus, the bed nucleus of the stria terminalis (BNST), amygdala, paraventricular nucleus of the thalamus (PVT), lateral septum (LS), and brainstem catecholamine cell groups. These populations both receive inputs from the mPFC and have been implicated in the control of PVN function during stress (e.g., Hurley et al., 1991; Sawchenko et al., 2000).

To investigate which of these populations might participate in mPFC modulation of PVN stress responses, we first determined whether mPFC lesions that increased PVN responses to a psychological stressor also elicited corresponding changes in activation of any of these brain regions. Changes in neuronal activation were indicated by alterations in expression of the immediate early gene protein product, Fos. Surprisingly, this study showed that lesions of the mPFC affected cell recruitment by air puff in only one of the candidate relay populations examined, the ventral (v) region of the BNST. The next step was therefore to better characterize the role of the BNST in the mpPVN CRF cell response to air puff with particular regard to its potential for integration of information from the mPFC to the PVN in response to stress. We investigated whether this candidate relay population directly innervates the PVN, as assessed by retrograde tracing, and whether there are any direct projections from the mPFC to the BNST that are recruited by air puff. We also examined the effects of BNST lesions on recruitment of the PVN and extra-hypothalamic cells in response to air puff.

MATERIALS AND METHODS

Subjects

All experiments were performed on adult male Wistar rats (250–550 g) according to protocols approved by the University of Queensland Animal Experimentation Ethics Committee. Animals were housed in individual chambers under standard laboratory conditions: ambient temperature 24°C, 12-hour light/dark cycle (lights on at 6:00), with pelleted food and water ad libitum. All surgery was conducted using sodium pentobarbital anesthesia (50 mg/kg, i.p., Nembutal, Rhone Merieux, Pinkenba, QLD, Australia).

Surgery: cortical and BNST ibotenic acid lesions

Bilateral lesions of the mPFC (n = 18) or BNST (n = 15) were made using the excitotoxin ibotenic acid. The animal was secured in a stereotaxic device and the skull exposed via a midline incision. A glass micropipette (tip diameter 20–25 μm) was then used to pressure inject ibotenic acid (50 nl per site, 5 ng/nl in 0.9% NaCl, Sigma Chemicals, Castle Hill, Australia) bilaterally into the appropriate brain region. For the mPFC, injections were made at 2.5 mm rostral and 0.7 mm lateral to bregma. To achieve lesions that encompassed both the prelimbic (PrL) and infralimbic (IL) regions of the mPFC, excitotoxin was injected at two sites: 4.0 and 5.0 mm ventral to skull surface. It has previously been found in this laboratory that it is exceedingly difficult to make a lesion that completely avoids the dBNST (Crane et al., 2003a); thus, we attempted to achieve lesions that encompassed both the dorsal and ventral regions of the BNST. Coordinates used were 0.0 and 0.2 mm caudal and 1.7 mm lateral to bregma and 6.5 mm ventral to skull surface. The micropipette was left in place for 5 minutes after injection to reduce diffusion of ibotenic acid back along the injection track. Each of the mPFC-lesioned and BNST-lesioned groups was processed at the same time as a separate group of sham-lesioned animals (mPFC-lesion study, n = 13; BNST-lesion study, n = 7). These animals underwent the same surgery, but the micropipette contained no ibotenic acid and no injection was made.

Because of the potential for changes in stress-induced PVN activation to result in changes in hypothalamic-pituitary-adrenal (HPA) axis activity, these animals were also prepared with vascular cannulae to allow collection of blood samples for subsequent determination of plasma hormone levels. Animals were fitted with a silastic-tipped vinyl cannula in the left femoral artery on the same day as the neurosurgery. The cannula was routed under the skin,

Abbreviations

IIIV	third ventricle
ac	anterior commissure
ACTH	adrenocorticotropic hormone
ANOVA	analysis of variance
apPVN	anterior parvocellular hypothalamic paraventricular nucleus
BNST	bed nucleus of the stria terminalis
CeA	central amygdala
CRF	corticotropin-releasing factor
CRF-IR	corticotropin-releasing factor-immunoreactivity
CTb	cholera toxin b subunit
CTb-IR	cholera toxin b subunit-immunoreactivity
dBNST	dorsal bed nucleus of the stria terminalis
DMH	dorsomedial hypothalamus
dpPVN	dorsal parvocellular hypothalamic paraventricular nucleus
f	fornix
Fos-IR	Fos-immunoreactivity
HPA	hypothalamic-pituitary-adrenal
ic	internal capsule
IL	infralimbic
lpPVN	lateral parvocellular hypothalamic paraventricular nucleus
LS	lateral septum
LV	lateral ventricle
MeA	medial amygdala
mgPVN	magnocellular hypothalamic paraventricular nucleus
mPFC	medial prefrontal cortex
mpPVN	medial parvocellular hypothalamic paraventricular nucleus
NTS	nucleus tractus solitarius
PrL	prelimbic
PVN	paraventricular nucleus of the hypothalamus
PVT	paraventricular nucleus of the thalamus
TH	tyrosine hydroxylase
vBNST	ventral bed nucleus of the stria terminalis
VLM	ventrolateral medulla
VMH	ventromedial hypothalamus

exteriorized dorsal to the scapulae, and capped. Each cannula was filled with anticoagulant heparinized saline (250 units/ml) containing antibiotic (20 mg/ml gentamicin; Parnell Laboratories, Alexandria, NSW, Australia). During the 7-day recovery period, the cannula was flushed every second day with gentamicin in heparinized saline.

Because there was some concern that a bilateral BNST lesion may cause an alteration of feeding behavior and/or body mass (Herman et al., 1994), food intake during the week postsurgery was monitored. The pelleted food was weighed at the end of 7 days and the amount subtracted from that allocated to the animal after surgery to determine the amount of food consumed. Each animal in the BNST lesion group was weighed just prior to surgery and again just prior to perfusion.

Surgery: PVN and BNST retrograde tracer injections

In a separate group of animals, the retrograde tracer cholera toxin b subunit (CTb; 1% solution in isotonic saline, List Biologicals, Campbell, CA) was iontophoretically deposited unilaterally either into the PVN, the dorsal (d) BNST only, or into both the dBNST and vBNST. Of the 18 animals that received CTb injections into the PVN, 10 were found to have deposits in the PVN, eight were excluded. Of the 12 animals that received CTb injections into the BNST, five were found to have appropriate deposits in the BNST, seven were excluded. Deposits were made using a 5-μm diameter glass micropipette (PVN coordinates: 1.5 mm caudal and 0.3 mm lateral to bregma and 7.0 mm ventral to brain surface, BNST coordinates 0.2 mm caudal and 1.4 mm lateral to bregma and 6.0 or 6.5 mm ventral to skull surface) by passing pulsed current (7 seconds on, 7 seconds off, 6 μA) for 20 minutes. The micropipette was kept in place for 10 minutes after injection to reduce diffusion of the CTb back along the injection track. These animals did not receive femoral artery cannulae.

Experimental setup: cortical and BNST lesion experiments

Seven days after surgery, cannulated animals had their femoral artery cannula attached via polyethylene tubing to a syringe outside the housing chamber, thus allowing blood sampling without handling. Animals were then left undisturbed for 90 minutes prior to exposure to air puff, which always occurred between 9:45 and 10:15 AM to minimize circadian rhythm-related variations in the stress response. Approximately half of the animals were not subjected to stress, but were otherwise treated identically to those exposed to air puff.

During the experiment, blood samples (0.45 ml, immediately replaced with an equal volume of heparinized saline) were collected from each animal 5 minutes before and 10, 30, 45, 60, and 90 minutes after onset of stressor application, or at equivalent time-points in the case of nonstressed controls. Blood samples were kept on ice until centrifuged and the plasma aliquots then stored at –20°C for subsequent radioimmunoassay to determine circulating ACTH concentrations.

Experimental setup: retrograde tracing experiments

Animals that had received CTb deposits directed at the PVN or BNST were all subjected to the same air puff protocol after a 7-day recovery period. These animals were not cannulated and therefore no blood samples were collected from these animals.

Stressor

The stressor used in this study, air puff, consisted of a series of 27 puffs of pressurized air (300 kPa) directed at the head of the freely moving animal from a distance of 5–10 cm, delivered over a period of approximately 15 minutes. The air puffs were administered in nine blocks, each block consisting of three puffs of 2 seconds duration with 10 seconds between puffs and 1 minute between blocks.

Tissue fixation and sectioning

Two hours after the onset of stressor application, all animals were deeply anesthetized with sodium pentobarbitone (80 mg/kg, i.p., Nembutal) and perfused transcardially with sodium nitrite solution (2% in 0.1 M phosphate buffer (PB), pH 7.4), followed by 4% formaldehyde (500 ml in 0.1 M PB, pH 7.4). After perfusion, brains were immediately removed and postfixed for 2 hours at 4°C in the same 4% formaldehyde solution and cryoprotected overnight in 10% sucrose (in PBS, 4°C). Serial coronal forebrain (40 μm) and brainstem (50 μm) sections were then cut using a freezing microtome.

Immunocytochemistry

Patterns of Fos expression and either cell phenotype or retrograde labeling were determined using a previously documented dual immunoperoxidase technique (Smith and Day, 1993; Smith et al., 1995; Buller et al., 1999). Neuronal activation was assessed on the basis of Fos-immunoreactivity (Fos-IR), seen as a black deposit in the nucleus. Cell phenotype was determined by immunoreactivity to antibodies directed against either CRF or tyrosine hydroxylase (TH; a marker of catecholamine synthesis), seen as amber staining of the cytoplasm. Neurons projecting to the PVN or BNST as appropriate were identified by CTb-immunoreactivity (CTb-IR), also seen as amber staining of the cytoplasm.

Briefly, a 1-in-4 series of forebrain sections and (for the lesion experiments only) a 1-in-5 series of brainstem sections taken from each animal were incubated in primary Fos antibody (48 hours, 1:50,000 rabbit polyclonal, Santa Cruz, CA). The sections were next incubated in the secondary antibody (2 hours, 1:300 biotinylated donkey anti-rabbit, Jackson ImmunoResearch, West Grove, PA) and then in avidin–biotin–horseradish peroxidase complex solution (Vector Elite Kit, Burlingame, CA) for a further 2 hours. The sections were subsequently incubated in nickel diaminobenzidine to visualize the horseradish peroxidase activity, yielding a black nuclear deposit. The reaction was terminated once an optimal contrast between specific cellular and nonspecific background labeling was reached.

To visualize cytoplasmic immunoreactivity and thus establish phenotype in the lesion experiments, forebrain sections were incubated in antibodies to CRF (36 hours, 1:25,000 rabbit polyclonal; Peninsula Laboratories, Belmont CA), while brainstem sections were incubated in antibodies to TH (36 hours, 1:40,000 monoclonal; Incstar, Stillwater, MN). For animals that had received retrograde tracer deposits, forebrain sections were incubated in antibodies to CTb (36 hours, 1:15,000 goat polyclonal; List Biologicals, Campbell, CA). The sections were then incu-

bated for 2 hours in biotinylated donkey secondary antibodies as appropriate: antirabbit for CRF (1:400, Jackson ImmunoResearch), antimouse for TH (1:400, Jackson ImmunoResearch), or antisheep for CTb (1:400, Jackson ImmunoResearch), followed by a further 2 hours incubation in an avidin–biotin–horseradish peroxidase complex solution (Vector Elite Kit). To visualize horseradish peroxidase activity, sections were then incubated in diaminobenzidine (nickel omitted) and the reaction terminated when optimal contrast between specific cellular labeling and nonspecific background labeling was achieved. To minimize variations in immunolabeling, sections from each experimental group were processed simultaneously. Sections were mounted on chrome alum-coated slides, dehydrated in a series of alcohols, cleared in xylene, and coverslipped.

Radioimmunoassay

To determine plasma concentrations of ACTH from each experimental group, a radioimmunoassay (ICN Biomedicals, Orangeburg, NY) was performed. All samples were assayed together, with an intraassay coefficient of variation less than 10%. The lower limit of detection was 10 pg/ml.

Analysis

Placement of mPFC and BNST lesions was assessed on the basis of gliosis and neuronal cell loss in a 1-in-4 series of Nissl-stained forebrain sections and also on the basis of reduction of numbers of Fos-IR cells in the mPFC or dBNST and vBNST as appropriate. The mPFC was defined as the region medial to the corpus callosum as described previously (Hurley et al., 1991). For the BNST, regions above the anterior commissure were defined as dBNST and those below the anterior commissure as vBNST, the boundaries being defined on the basis of Nissl-stained sections and previously reported cytoarchitectural differences (Ju and Swanson, 1989; Moga et al., 1989).

An experimenter, blind to the experimental condition, performed counts of cells positive for Fos-IR. In the lesion experiments, Fos-IR nuclei within the anterior parvocellular (ap) PVN, dorsal parvocellular (dp) PVN, lateral parvocellular (lp) PVN, and magnocellular (mg) PVN were counted over two rostrocaudal levels, within the dorsomedial hypothalamus (DMH) and ventromedial hypothalamus (VMH) over six rostrocaudal levels, and within the mpPVN over three rostrocaudal levels, 160 μm apart (Buller et al., 2003). A tendency towards increased Fos expression in the mpPVN led to an examination of numbers of Fos-IR cells colocalizing CRF-immunoreactivity (CRF-IR). These were counted within the mpPVN over two rostrocaudal levels, 160 μm apart. In addition, for the lesion experiments Fos-IR nuclei within the dBNST and vBNST were counted over four rostrocaudal sections, 160 μm apart. Fos-IR nuclei within the PrL and IL regions of the mPFC, the central (CeA), and the medial (MeA) amygdala were counted over five rostrocaudal levels, and in the PVT over seven rostrocaudal sections at 160 μm intervals. Fos-IR nuclei within the ventral LS (LSV) were counted over five rostrocaudal sections 320 μm apart. In the brainstem, Fos-IR cells colocalizing TH-like immunoreactivity were counted in the nucleus tractus solitarius (NTS) and ventrolateral medulla (VLM) from 2.5 mm caudal to 1.5 mm rostral to obex, at 250-μm intervals. In experiments where animals had received retrograde tracer deposits of CTb into the PVN, numbers of Fos-IR cells colocalizing CTb-IR were counted in the dBNST and vBNST over four rostrocaudal sections, 160 μm apart. Where animals had received retrograde tracer into the BNST, numbers of Fos-IR cells colocalizing CTb-IR were counted in the mPFC over five sections at 160-μm intervals.

As preliminary analysis indicated that the Fos-IR cell counts and ACTH values did not display homogeneity of variance, raw values were transformed as appropriate using a log or square root transformation before statistical analysis to achieve a normal distribution. Data analysis was performed using commercial statistics software packages (Instat 2.03 for Macintosh, GraphPad Software 1994 and Statistica 4.1, Stat/Soft, Tulsa, OK). All data are expressed as the mean ± SEM. Statistical significance was assumed when $P < 0.05$. Comparisons were performed between the numbers of Fos-IR nuclei within a specific brain region using a two-way analysis of variance (ANOVA) with lesion and stress as between factors. Where a significant interaction was found, a one-way ANOVA was performed followed, where significant, by a Student-Newman-Keuls post-hoc comparison. Comparisons of plasma ACTH concentrations were made using a three-way ANOVA with lesion and stress as the between factors and time as the repeated measure nested within animals. Where a significant interaction was found, a two-way ANOVA was performed at each time point with lesion and stress as the between factors and, given a significant interaction, a one-way ANOVA was then carried out at each time point followed by a Student-Newman-Keuls post-hoc comparison.

Images for publication were adjusted for brightness and contrast in Adobe PhotoShop 8.0 (Adobe Systems, San Jose, CA) and composed for publication in Adobe Illustrator 11.0.

RESULTS

Effects of mPFC lesions

Effects of air puff on sham-lesioned animals. Compared with nonstressed sham-lesioned animals (n = 8), which displayed negligible numbers of Fos-IR neurons, exposure to air puff was associated with a significant increase in Fos-IR cell numbers in all regions counted, i.e., a significant main effect of stressor was seen with a two-way ANOVA (Table 1). Sham-lesioned animals subjected to air puff stress (n = 5) displayed patterns of Fos-IR neurons typical of those described previously for air puff-stressed animals (Duncan et al., 1996; Palmer and Printz, 1999; Spencer et al., 2004) as well as for animals subjected to other types of psychological stressor. In accordance with a profile typical of other psychological stressors, such as restraint and noise (Abraham and Kovacs, 2000; Dayas et al., 2001),, in both the NTS and VLM peak numbers of Fos-IR TH cells were seen well caudal to the level of the obex. The majority of the activated TH cells in the NTS were situated 0.25–1.5 mm caudal to obex, a region containing predominantly noradrenergic (A2) cells. Similarly, the majority of the activated VLM TH cells were situated in the noradrenergic (A1) region, 0.75–2.25 mm caudal to obex (data not shown).

Exposure to air puff caused a significant increase in numbers of Fos-IR cells in both the MeA and CeA relative to nonstressed animals. This increase was considerably

TABLE 1. Effects of mPFC lesions on numbers of Fos-IR cells seen in response to air puff

Neuronal population	Sham-lesion		mPFC-lesion	
	No stressor (n = 8)	Air puff (n = 5)	No stressor (n = 9)	Air puff (n = 9)
mPFC				
PrL	21 ± 8	448 ± 77*	8 ± 4	35 ± 14**
IL	14 ± 7	218 ± 40**	2 ± 1	10 ± 6**
PVN				
PVN total	28 ± 13	340 ± 80	33 ± 8	435 ± 50
apPVN	7 ± 3	114 ± 39	9 ± 3	102 ± 23
dpPVN	3 ± 1	21 ± 2	2 ± 0	25 ± 6
lpPVN	3 ± 2	9 ± 4	1 ± 1	14 ± 3
mgPVN	3 ± 2	33 ± 11	5 ± 2	55 ± 10
mpPVN	13 ± 6	162 ± 32	15 ± 4	238 ± 26
mpPVN CRF cells	1 ± 0	66 ± 18**	1 ± 0	174 ± 39**
DMH	15 ± 7	301 ± 48	24 ± 7	319 ± 47
VMH	50 ± 21	161 ± 43	67 ± 18	234 ± 50
Amygdala				
CeA	22 ± 5	204 ± 27	36 ± 11	143 ± 29
MeA	50 ± 17	473 ± 65	98 ± 42	577 ± 43
BNST				
dBNST	3 ± 1	23 ± 5	9 ± 3	29 ± 5
vBNST	16 ± 1	314 ± 71**	19 ± 3	604 ± 77**
PVT	133 ± 13	333 ± 43	196 ± 24	335 ± 59
LSV	21 ± 9	160 ± 35	21 ± 7	192 ± 34
Brainstem				
NTS TH cells	19 ± 7	150 ± 37	49 ± 13	118 ± 22
VLM TH cells	15 ± 6	92 ± 15	30 ± 11	103 ± 17

Air puff exposure was associated with a significant increase in numbers of Fos-IR cells in all the cell populations counted (significant main effect of stressor with two-way ANOVA for each brain region). However, post-hoc tests were only performed where a significant interaction with lesion was also found.
*$P < 0.01$; **$P < 0.001$.
[a]Airpuff-exposed versus nonstressed animals.
[b]mPFC-lesioned versus sham-lesioned animals. Compared with sham-lesioned animals, lesions of the mPFC had no effect on the number of Fos-IR neurons seen in nonstressed animals in any of the brain regions examined. Lesions of the mPFC did result in a significant reduction in the number of air puff-induced Fos-IR cells in the mPFC. Also, significantly greater numbers of Fos-IR mpPVN CRF cells and vBNST cells were seen in mPFC-lesioned animals after air puff than in sham-lesioned animals exposed to the same air puff.

greater, however, in the MeA than in the CeA (Table 1). Very few Fos-IR cells were observed in any other divisions of the amygdala after air puff. Exposure to air puff also resulted in a significant increase in numbers of Fos-IR cells seen in the dBNST and vBNST relative to nonstressed animals. In the dBNST, the Fos-IR cells were seen particularly in the dorsal lateral region, with very few in the anterior lateral and the juxtacapsular regions. The greatest increase in Fos-IR cells was seen in the vBNST, particularly located in the ventral medial and parastrial regions. Air puff elicited robust activation of the PrL and IL regions of the mPFC (Table 1), while the anterior cingulate and dorsal peduncular regions showed virtually no activation. The greatest number of Fos-IR cells seen in the mPFC after air puff was present in layers VI and V. Furthermore, the numbers of Fos-IR cells observed in response to air puff were not different between the left and right hemispheres (data not shown). Animals exposed to air puff also displayed substantially greater numbers of Fos-IR cells in the various divisions of the PVN, including in the CRF cells of the mpPVN than did nonstressed animals (Table 1). Exposure to air puff also resulted in a significant increase in numbers of Fos-IR cells seen in the DMH, VMH, PVT, and LSV relative to nonstressed animals (Table 1).

Characterization of mPFC lesions. Light microscope examination of Nissl-stained sections from animals that had received mPFC-directed injections of ibotenic acid revealed substantial cell loss and gliosis throughout all of the PrL and most of the IL regions of the mPFC, with some damage to the cingulate area (Fig. 1A,B). These lesions extended over almost the entire rostrocaudal length of the mPFC, from 2.2–3.7 mm rostral to bregma (Fig. 1C). In contrast to sham-lesioned animals, which displayed substantial numbers of Fos-IR cells in the PrL and IL regions in response to air puff, almost no Fos-IR cells were visible in the mPFC of air puff-stressed lesioned animals (n = 9; Fig. 1D,E; Table 1). The number of PrL Fos-IR cells seen with air puff was reduced by 92 ± 3% ($F_{(3,27)} = 11.0$, $P < 0.001$) and the IL by 95 ± 3% ($F_{(3,27)} = 18.4$, $P < 0.0001$) compared with the appropriate means for the sham-lesioned animals.

Effects of mPFC lesions on responses to air puff. In comparison with sham-lesioned animals, mPFC lesions (n = 9) had no significant effect on neuronal activation in nonstressed animals (Table 1). Lesions of the mPFC did, however, alter certain responses in animals subjected to air puff. Air puff-exposed animals with mPFC lesions displayed a tendency towards a greater number of Fos-IR mpPVN cells. Because the mpPVN is known to contain a significant population of stress-sensitive CRF cells, Fos-IR CRF cells in the region were also counted. The mPFC lesion significantly increased the number of activated CRF cells in the mpPVN ($F_{(3,27)} = 130.2$, $P < 0.0001$) compared with sham-lesioned animals subjected to the same stressor (Table 1; Fig. 2). In light of this finding, previously collected blood samples were assayed for plasma ACTH. Compared with nonstressed animals, air puff also produced a significant elevation in plasma ACTH, i.e., a significant main effect of stress and time with a three-way ANOVA. Despite the effects on mpPVN CRF cell Fos expression, mPFC lesions did not significantly alter plasma ACTH responses to air puff (Fig. 3). As no significant interaction between stress, lesion, and time was found, post-hoc tests were not performed. The mPFC lesions also significantly enhanced numbers of Fos-IR cells seen in the vBNST after air puff ($F_{(3,27)} = 152.9$, $P < 0.0001$) compared with sham-lesioned animals (Table 1; Fig. 4). None of the other candidate relay populations examined was significantly affected by the lesion (Table 1).

Examination of other potential relay sites between the mPFC and the mpPVN; the parabrachial nucleus, locus coeruleus, hippocampus, suprachiasmatic nucleus, and dorsal LS revealed very few Fos-IR cells after air puff in either the sham- or mPFC-lesioned animals in these populations. Formal counts of these regions were therefore not performed.

Effects of BNST lesions

Effects of air puff on sham-lesioned animals. As previously described for the sham-lesioned animals in the mPFC-lesioned group, the nonstressed sham-lesioned animals in the BNST-lesioned group (n = 3) displayed negligible numbers of Fos-IR neurons. Also, exposure to air puff was associated with similar increases in Fos-IR cell numbers in sham-lesioned animals in the BNST-lesioned group (n = 4) as in sham-lesioned animals in the mPFC-lesioned group. Except where the tendency for air puff to increase Fos-IR cell numbers in the sham-lesioned dBNST and lpPVN were not large enough to produce a significant main effect, a significant main effect of stressor was seen with a two-way ANOVA in the BNST-lesioned group in all regions counted (Table 2).

Characterization of BNST lesions. Examination of Nissl-stained BNST sections from the animals that had

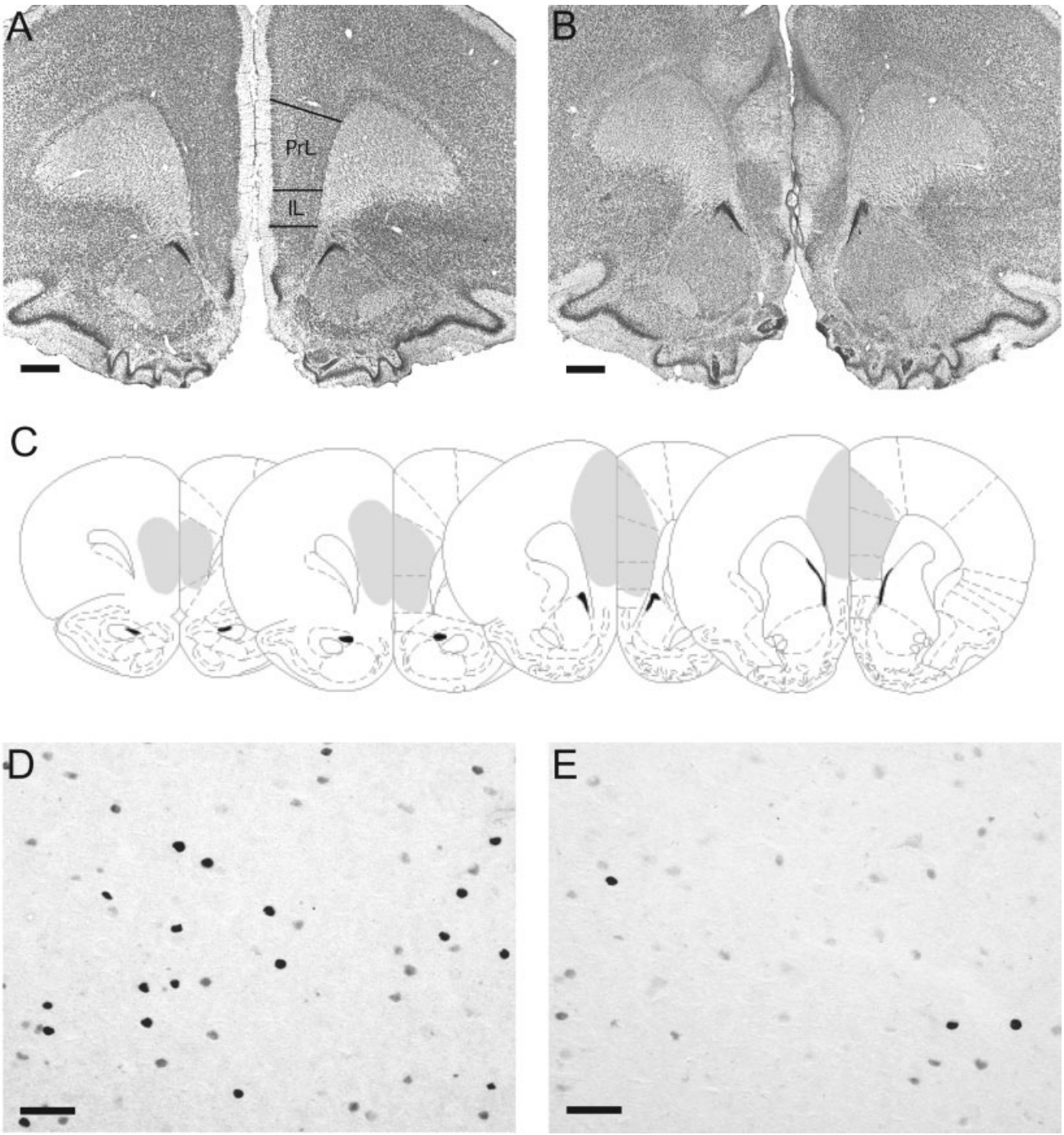

Fig. 1. Ibotenic acid caused substantial cell loss and gliosis in the PrL and IL regions of the mPFC. **A,B:** Photomicrographs of coronal sections through the PFC of (A) a sham-lesioned animal and (B) a mPFC-lesioned animal, Nissl-stained to visualize the location of the mPFC lesions. Neuronal cell loss is clearly evident, with gliosis extending into the IL region on the right-hand side. **C:** A schematic representation of the rostrocaudal extent of the mPFC lesion, adapted from camera lucida drawings of the mPFC of the animal depicted in B. Numbers indicate the distance in mm rostral to bregma. **D,E:** Photomicrographs of coronal mPFC sections of (D) a sham-lesioned animal and (E) an mPFC-lesioned animal immunolabeled for Fos. In contrast to sham-lesioned animals, almost no Fos-IR cells were visible in the mPFC of animals lesioned with ibotenic acid. IL, infralimbic; PrL, prelimbic. Scale bars = 500 μm in A,B; 50 μm in D,E.

received BNST-directed ibotenic acid injections revealed little obvious cell damage throughout the BNST. However, the more obvious cell loss occurred in the ventral medial, posterior lateral, and ventral lateral subnuclei with damage also apparent in the dorsal lateral, anterior lateral, and juxtacapsular subnuclei. The inclusion of each animal

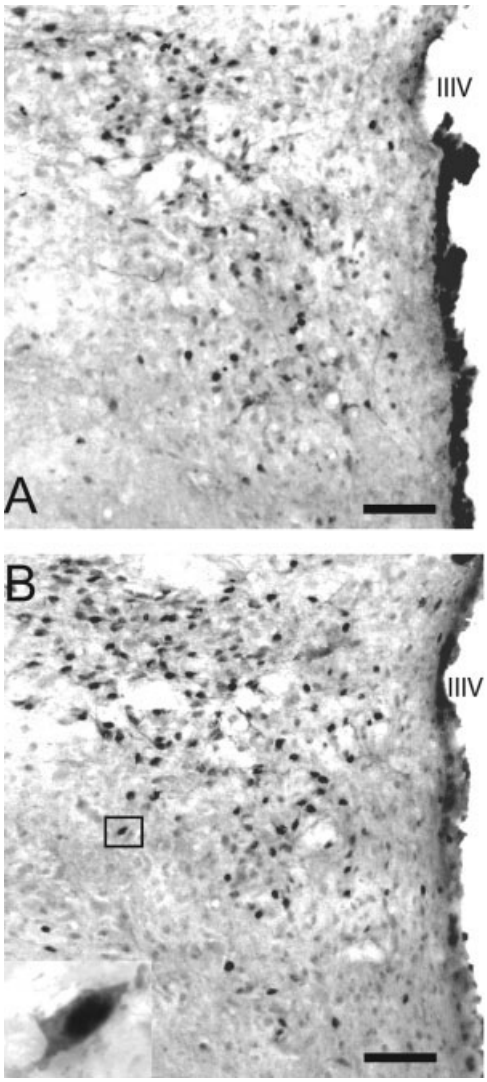

Fig. 2. Effect of mPFC lesions on expression of Fos in mpPVN CRF cells after air puff. Sham-lesioned animals (**A**) had fewer Fos-IR CRF cells within the mpPVN after air puff than mPFC-lesioned animals (**B**). Inset: Higher magnification photomicrograph of a representative Fos-IR CRF cell. Photomicrographs are from the left mpPVN. IIIV, third ventricle. Scale bars = 100 μm.

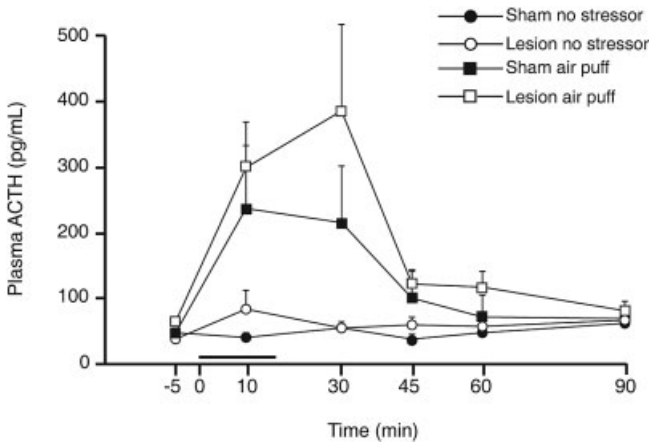

Fig. 3. Plasma ACTH responses to air puff in sham and mPFC-lesioned animals. Air puff (black bar) caused a significant increase in plasma ACTH concentrations in both mPFC-lesioned and sham-lesioned animals relative to nonstressed controls (significant main effect of stress and time with a three-way ANOVA). Lesions of the mPFC had no significant effect on basal plasma ACTH in nonstressed animals or on plasma ACTH responses to air puff relative to that of sham-lesioned animals.

in further analyses as a lesioned animal was therefore based on a functional effect on the BNST, i.e., a reduction in neuronal activation in the dBNST and vBNST as assessed by numbers of Fos-IR cells seen compared to sham-lesioned animals (Fig. 5).

Counts of Fos-IR cells in the dBNST and vBNST revealed a substantial reduction in response to air puff (dBNST = 68 ± 8% reduction; vBNST = 69 ± 5% reduction) in 11 of the 15 air puff-exposed, lesioned animals compared with the sham-lesioned animals, although a significant interaction between the lesion and stressor was only found with the two-way ANOVA in the case of the vBNST ($F_{(3,18)} = 12.7$, $P < 0.0001$). The remaining four animals displayed no changes in Fos-IR cell numbers. These latter were therefore excluded from further analysis as the lesions were judged to be ineffective. The reduction in numbers of Fos-IR cells in successfully lesioned animals was in every case very similar in the left and right hemispheres (data not shown).

Effects of BNST lesions on food intake and body mass. Lesions of the BNST had no effect on either the animals' food intake or their body mass. Sham-lesioned animals consumed 143 ± 10 g of pelleted rat chow in the 7 days after surgery, while BNST-lesioned animals ate 155 ± 6 g. Both sham and BNST-lesioned animals showed negligible body mass changes in the week after surgery. Sham-lesioned animals lost 2 ± 6 g in body mass, while BNST-lesioned animals lost 4 ± 4 g.

Effects of BNST lesions on responses to air puff. Compared with sham-lesioned animals, no effect was seen of the BNST lesions (n = 4) on Fos expression in non-stressed animals in any of the brain regions examined (Table 2). A trend towards a decrease in the number of Fos-IR cells was observed in the BNST, particularly the dBNST, but this did not prove to be significant.

There was a significant main effect of the BNST lesion (n = 11), resulting in a reduction in air puff-induced Fos-IR cell numbers in many of the brain regions examined compared with sham-lesioned animals exposed to air puff (Table 2). However, post-hoc tests were only performed where a significant interaction with air puff was also found. The number of Fos-IR CRF cells seen in the mpPVN after air puff was reduced by 87 ± 3% by the BNST lesions ($F_{(3,18)} = 25.7$, $P < 0.0001$). In consideration of this finding, blood samples were assayed for plasma ACTH. Compared with nonstressed animals, air puff also produced a significant elevation in plasma ACTH in the BNST-lesioned animals, i.e., a significant main effect of stress and time with a three-way ANOVA. Despite the reduction in mpPVN CRF cell activation with the BNST lesions, the tendency for the lesions to reduce the air puff-induced plasma ACTH increase did not achieve significance (Fig. 6) As no significant interaction between stress, lesion, and time was found, post-hoc tests were not

performed. Fos-IR cell numbers were also substantially reduced in the mPFC ($F_{(3,18)} = 21.7$, $P < 0.0001$), MeA ($F_{(3,18)} = 19.0$, $P < 0.0001$), CeA ($F_{(3,18)} = 4.3$, $P < 0.05$) and apPVN ($F_{(3,18)} = 31.5$, $P < 0.0001$; Table 2).

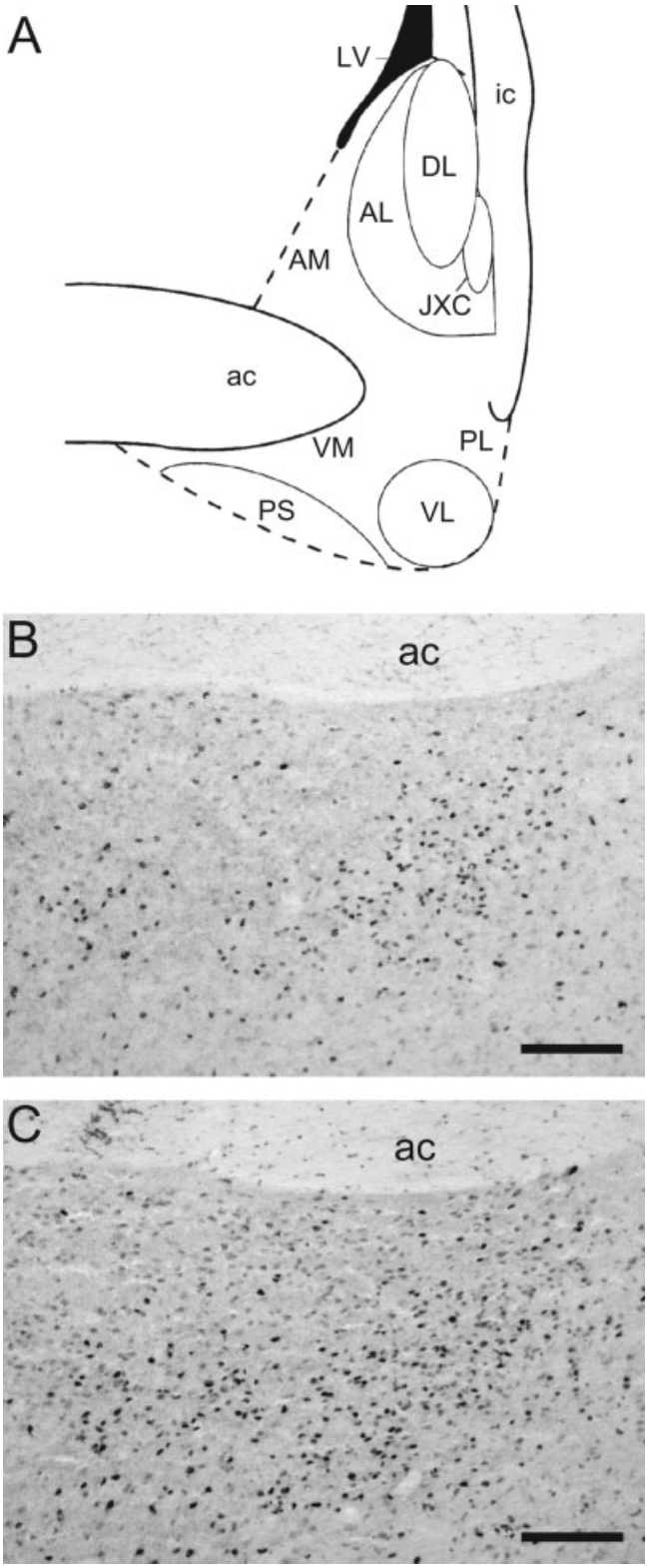

Effects of air puff on neurons projecting to the PVN

Of the 18 animals that received intracerebral CTb applications seven days prior to air puff exposure, 10 were found to have significant tracer deposits in the mpPVN (Fig. 7A). The extent to which the tracer was confined to the mpPVN varied. In four animals, CTb had spread from the mpPVN into the anterior magnocellular division. In another two animals, CTb had spread from the mpPVN into immediately caudal and dorsal areas. However, despite these variations in deposit sites, all 10 animals displayed large numbers of retrogradely labeled neurons in the ipsilateral vBNST, particularly in the parastrial and ventral medial regions (88 ± 13; Fig. 7B), but virtually no CTb-labeled cells in the contralateral vBNST or in the dBNST. Of the vBNST neurons expressing Fos ipsilateral to the CTb injection site (176 ± 19), 14 ± 1% proved to also be CTb-positive. The majority of the CTb-IR and double-labeled cells within the vBNST were seen just ventral to the anterior commissure (Fig. 7B).

Although the focus of this tracing experiment was to determine whether mpPVN-projecting vBNST cells were sensitive to psychological stress, we also inspected the mPFC in these animals. Deposits of CTb in the mpPVN failed to retrogradely label any cells in the mPFC.

Effects of air puff on neurons projecting to the dBNST and vBNST

Of the 12 animals that received retrograde tracer deposits into the BNST, five were found to have tracer deposits appropriately localized in the dBNST or the dBNST and vBNST. The degree of spread varied with two animals having tracer deposits in the dorsal and ventral BNST (Fig. 8A). In these animals, tracer was deposited predominantly in the caudal half of the BNST, with some spread slightly caudal to the target region. In one of these animals with dorsal and ventral BNST tracer, the CTb deposit was located in the ventral lateral and ventral medial subnuclei and in the dorsal lateral and anterior lateral and juxtacapsular regions with a little spread into the anterior medial region. In the other example, the deposit was found again in the ventral lateral and ventral medial subnuclei, in this case little deposit was found in the dorsal lateral BNST, but some CTb was present in the anterior lateral and anterior medial subnuclei. A further three of the 12 animals had retrograde tracer deposited discretely into the dorsal lateral, anterior lateral, and juxtacapsular subnuclei of the dBNST (Fig. 8B). In two of these cases the tracer was confined to the dBNST and was found throughout the whole of the dBNST. One animal had CTb that also extended caudal to the dBNST and in this case some of the anterior medial subnucleus also contained tracer.

Fig. 4. Effect of mPFC lesions on expression of Fos protein in the vBNST after air puff. A schematic diagram depicting the location and subdivisions of the BNST (**A**). Sham-lesioned animals (**B**) had fewer Fos-IR CRF cells within the vBNST after air puff than mPFC-lesioned animals (**C**). Photomicrographs are from the right vBNST. ac, anterior commissure; AL, anterior lateral; AM, anterior medial; DL, dorsal lateral; ic, internal capsule; JXC, juxtacapsular; LV, lateral ventricle; PL, posterior lateral; PS, parastrial; VL, ventral lateral; VM, ventral medial. Scale bars = 100 μm.

TABLE 2. Effects of BNST lesions on numbers of Fos-IR cells seen in response to air puff

Neuronal population	Sham-lesion		BNST-lesion	
	No stressor (n = 3)	Air puff (n = 4)	No stressor (n = 4)	Air puff (n = 11)
BNST				
dBNST	20 ± 7	40 ± 11	14 ± 5	16 ± 4
vBNST	72 ± 35	387 ± 87**	72 ± 6	126 ± 20***
PVN				
PVN total	43 ± 6	686 ± 123***	37 ± 5	161 ± 20***
apPVN	6 ± 2	328 ± 100***	14 ± 4	57 ± 10***
dpPVN	2 ± 1	22 ± 3	4 ± 3	14 ± 3
lpPVN	1 ± 1	5 ± 1	1 ± 1	5 ± 2
mgPVN	8 ± 2	35 ± 7	5 ± 2	21 ± 5
mpPVN	26 ± 6	297 ± 50	14 ± 4	65 ± 8
mpPVN CRF cells	5 ± 2	173 ± 30***	4 ± 2	27 ± 6***
DMH	28 ± 7	310 ± 81	25 ± 5	140 ± 17
VMH	67 ± 4	291 ± 55	70 ± 16	96 ± 15
mPFC	141 ± 75	2498 ± 613***	177 ± 38	987 ± 167**
Amygdala				
CeA	26 ± 14	177 ± 79[a]	35 ± 9	44 ± 11[b]
MeA	58 ± 22	589 ± 109***	69 ± 16	206 ± 31***
PVT	166 ± 60	534 ± 108	218 ± 57	264 ± 32
LSV	26 ± 6	282 ± 84	28 ± 8	190 ± 28
Brainstem				
NTS TH cells	25 ± 18	257 ± 44	20 ± 8	59 ± 13
VLM TH cells	1 ± 0.3	285 ± 67	1 ± 1	71 ± 13

Air puff exposure was associated with a significant increase in numbers of Fos-IR cells in all the cell populations counted except in the dBNST and lpPVN (significant main effect of stressor with two-way ANOVA for each brain region). A significant main effect of the lesion was found in the dBNST, the total PVN, mgPVN, mpPVN, mpPVN CRF cells, vBNST, and VMH. However, post-hoc tests were only performed where a significant interaction between the stressor and lesion was found. *$P < 0.05$; **$P < 0.01$; ***$P < 0.001$.

[a]airpuff-exposed versus nonstressed animals.

[b]BNST-lesioned versus sham-lesioned animals. Compared with sham-lesioned animals, lesions of the BNST had no significant effect on the numbers of Fos-IR neurons seen in nonstressed animals in any of the brain regions examined. Lesions of the BNST did result in a significant reduction in air puff-induced neuronal activation in the mpPVN CRF cells as well as in other brain regions examined compared with sham-lesioned animals.

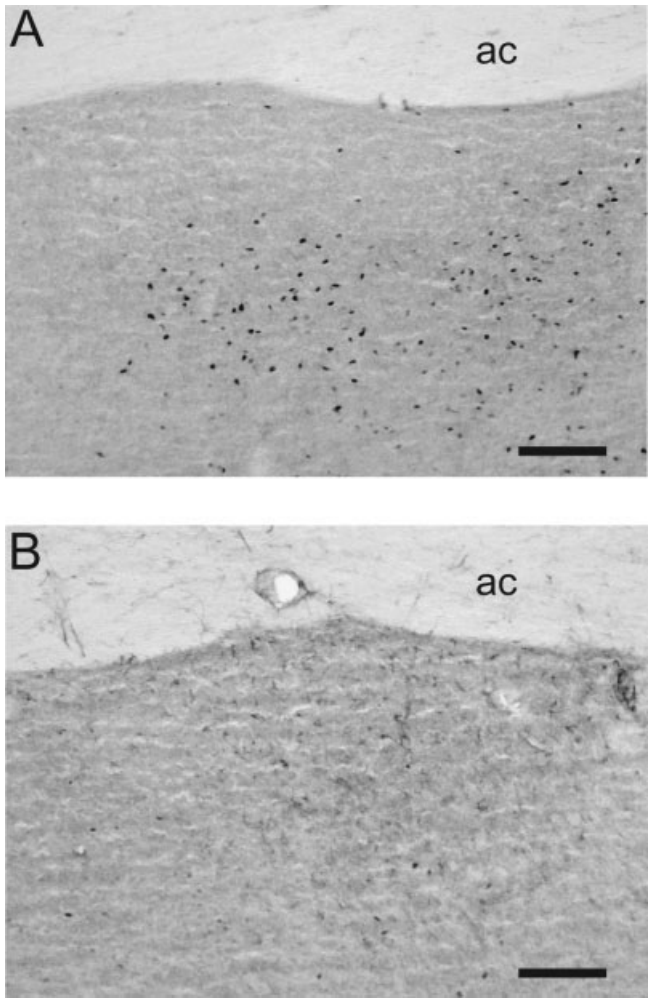

Fig. 5. Ibotenic acid caused a reduction in numbers of Fos-IR cells in both the dBNST and vBNST. **A,B:** Photomicrographs of coronal sections through the vBNST of (A) a sham-lesioned animal and (B) a BNST-lesioned animal immunolabeled for Fos. In contrast to sham-lesioned animals, few Fos-IR cells were visible in the BNST of animals lesioned with ibotenic acid. Photomicrographs are from the right vBNST. ac, anterior commissure. Scale bars = 100 μm.

Very few retrogradely labeled neurons were identified in the mPFC of animals in which the tracer had been discretely deposited in the dBNST only. The CTb-IR cells that were identified were seen exclusively in the deeper layers V and VI and almost exclusively ipsilateral to the tracer injection site (ipsilateral 7 ± 6; contralateral 2 ± 2).

The example where the dBNST CTb deposit extended caudal to the BNST showed a profile more similar to those with vBNST deposits. In these animals substantial numbers of retrogradely labeled cells were seen in the mPFC, again predominantly ipsilateral to the tracer deposit (ipsilateral = 388 ± 121; contralateral, 52 ± 35). The majority of these were located in the middle to deep layers, with the greatest density being in the IL region (Fig. 8C). Of the Fos-IR cells of the mPFC seen after air puff (1,500 ± 181), a negligible number was found to also be retrogradely labeled from the vBNST (Fig. 8C).

DISCUSSION

The present study demonstrates the importance of both the mPFC and the BNST in modulation of the mpPVN CRF cell response to air puff, and provides some suggestion that the mPFC may modulate such responses acting indirectly via the vBNST. Lesions of the mPFC enhanced the recruitment of mpPVN CRF cells by air puff stress. Importantly, this effect was accompanied by altered neuronal recruitment in only one of the candidate relay populations examined, the vBNST. Furthermore, lesions of the BNST resulted in a substantial reduction in neuronal activation with air puff in all regions examined. This study is therefore important in highlighting the significance of both the mPFC and BNST in influencing the response to a psychological stressor, air puff.

Choice of stressor

There is now considerable support for the view that the brain distinguishes at least two distinct categories of acute, unconditioned stressors: psychological, characterized by a threatened disturbance of the organism's current state; and physical, taking the form of an already realized disturbance of tissue integrity (Sawchenko et al., 1996, 2000; Herman and Cullinan, 1997; Dayas et al., 2001). The ability of the mPFC to suppress stress responses has been suggested to vary with the type of stressor. Originally it was thought that the mPFC suppresses responses only to psychological stressors (Diorio et al., 1993). However, it has recently been shown that mPFC lesions can potentiate responses to a physical stressor, immune chal-

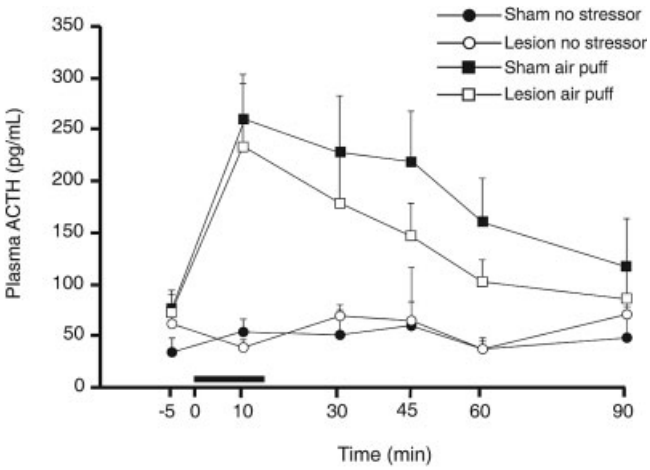

Fig. 6. Plasma ACTH responses to air puff in sham and BNST-lesioned animals. Air puff (black bar) caused a significant increase in plasma ACTH concentrations in both BNST-lesioned and sham-lesioned animals relative to nonstressed controls (significant main effect of stress and time with a three-way ANOVA). Lesions of the BNST had no significant effect on basal plasma ACTH in nonstressed animals or on plasma ACTH responses to air puff relative to that of sham-lesioned animals.

lenge (Crane et al., 2003b). It was subsequently suggested that stressor intensity may be of importance (Crane et al., 2003b), but a recent investigation involving two stressors of apparently similar intensity eliciting differential effects on mPFC-lesioned animals seems to argue against this conclusion (Figueiredo et al., 2003). Accordingly, the explanation of why the mPFC is effective in suppressing responses to some stressors but not others remains elusive. Nevertheless, for the purpose of the present study we deliberately chose a stressor that was both of moderate intensity, to avoid saturating the stress response, and characterized by the brain as psychological, in consideration of the majority of the existing evidence.

Previous reports suggested that air puff fulfils both of these requirements (Thrivikraman et al., 2000; Spencer et al., 2004) and the present findings validate that view. With regard to stressor intensity, the number of mpPVN CRF cells activated by air puff in this study was estimated at no more than 10% of the total and was ~25% of that encountered in past studies from this laboratory using stressors such as noise or restraint (Dayas et al., 2001).

With regard to the stressor type, it is evident that the brain classifies air puff as a psychological stressor. Thus air puff, just as previously reported for stressors such as noise, swim stress, and restraint (Abraham and Kovacs, 2000; Dayas et al., 2001), elicited amygdala Fos expression that was most prominent in the MeA, and medullary catecholamine cell Fos expression that peaked at levels caudal to the level of obex. This profile contrasts with physical stressors, such as hemorrhage and immune challenge, which are associated with Fos expression primarily in the CeA, and in subpopulations of medullary catecholamine cells centered at or just rostral to obex (Dayas et al., 2001). In the BNST with air puff, Fos-IR was seen predominantly in the ventral medial and parastrial subnuclei of the ventral BNST. There was little Fos-IR in the dorsal region and what was present was confined to the dorsal

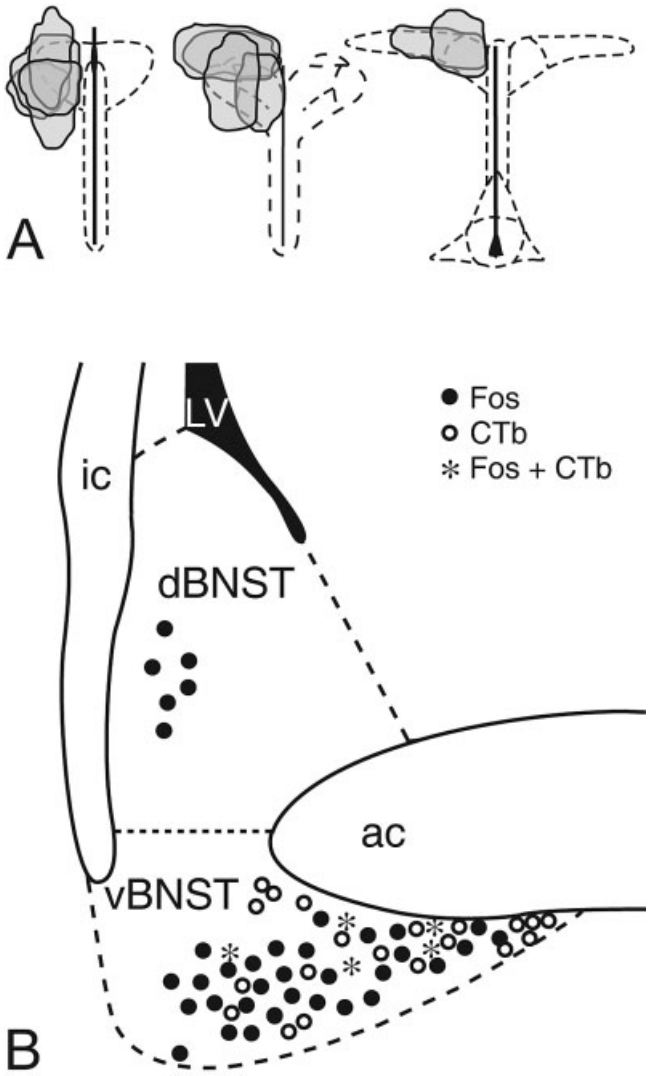

Fig. 7. Colocalization of retrograde tracer and Fos protein in vBNST cells of animals that had received mpPVN CTb deposits. **A:** A schematic representation of the successful PVN CTb deposit sites adapted from camera lucida drawings. **B:** A schematic coronal diagram illustrating the distribution of Fos-IR (filled circle), CTb-IR (open circle), and double-labeled (star) neurons in the BNST ipsilateral to the PVN CTb deposit in an animal subjected to air puff. One symbol corresponds to one cell. ac, anterior commissure; CTb, cholera toxin b subunit; dBNST, dorsal bed nucleus of the stria terminalis; ic, internal capsule; LV, lateral ventricle; PVN, hypothalamic paraventricular nucleus; vBNST, ventral bed nucleus of the stria terminalis. Scale bar = 100 μm.

lateral region. This profile is in contrast to that shown by animals exposed to a physical stressor. For instance, the physical stressor immune challenge has been shown to induce strong Fos-IR in the dorsal lateral subnucleus of the dBNST and substantial Fos-IR is also seen in the ventral lateral region as well as in the ventral medial and parastrial regions (Crane et al., 2003a). The profile of Fos expression seen here with air puff clearly mimics that of other psychological stressors. It is therefore apparent that air puff is categorized by the brain as a psychological stressor.

Role of the mPFC in mpPVN CRF cell responses to air puff

Previous studies have shown that disruption of mPFC function can alter a variety of responses to stress (Diorio et al., 1993; Espejo and Minano, 1999; Sullivan and Gratton, 1999; Brake et al., 2000; Lacroix et al., 2000; van Eden and Buijs, 2000; Crane et al., 2003b). Thus, as outlined in the Introduction, many autonomic, behavioral, and hormonal responses to stress are potentially inhibited by activation of the mPFC. The PVN is commonly accepted to have a preeminent role in integrating stress responses and there is evidence to suggest that the mPFC can suppress certain PVN responses to stress (Figueiredo et al., 2003). The results presented in this investigation demonstrate that the mPFC suppresses certain PVN responses to air puff, particularly the expression of Fos protein by mpPVN CRF cells.

Perhaps surprisingly, the increase in numbers of stress-activated mpPVN CRF cells seen here with the mPFC lesion was not accompanied by a corresponding change in the stress-induced ACTH responses. With respect to HPA axis control, it is increasingly accepted that the HPA axis does not necessarily operate in a simple chain reaction (Ehrhart-Bornstein et al., 1998; Pignatelli et al., 1998; Bornstein and Chrousos, 1999). It must be noted that ACTH release from the anterior pituitary is not controlled exclusively by CRF. An increase in the number of activated CRF cells may be compensated for by a corresponding decrease in the release of other secretagogues such as oxytocin, arginine vasopressin (Whitnall, 1993), and noradrenaline (Watanabe et al., 1991). An upregulation in the number of CRF cells of the mpPVN stimulated by a stressor could also result in a compensatory decrease in the amount of CRF released from each active cell. Although a major function of the mpPVN CRF cells is to stimulate ACTH release from the anterior pituitary and so stimulate glucocorticoid release from the adrenal cortex (Whitnall, 1993), not all mpPVN CRF cells are involved in HPA axis regulation. Corticotropin-releasing factor cells of the mpPVN stimulate noradrenaline synthesis and release in the brainstem, chiefly from the locus coeruleus, in response to stress, thus modulating a variety of autonomic functions such as gastric motility (Tache et al., 1993; Black, 1994). Thus, while the absence of a measurable change in stress-induced ACTH with the mPFC lesion was a little surprising, we believe that the increased recruitment of mpPVN CRF cells stands as valid and interesting evidence of an altered response of the brain to the psychological stressor, air puff.

Interestingly, other investigations have demonstrated a potentiation of the release of ACTH with psychological stress in animals with mPFC lesions (Diorio et al., 1993; Figueiredo et al., 2003). Indeed, the trend in the present study was for an increase in air puff-induced ACTH re-

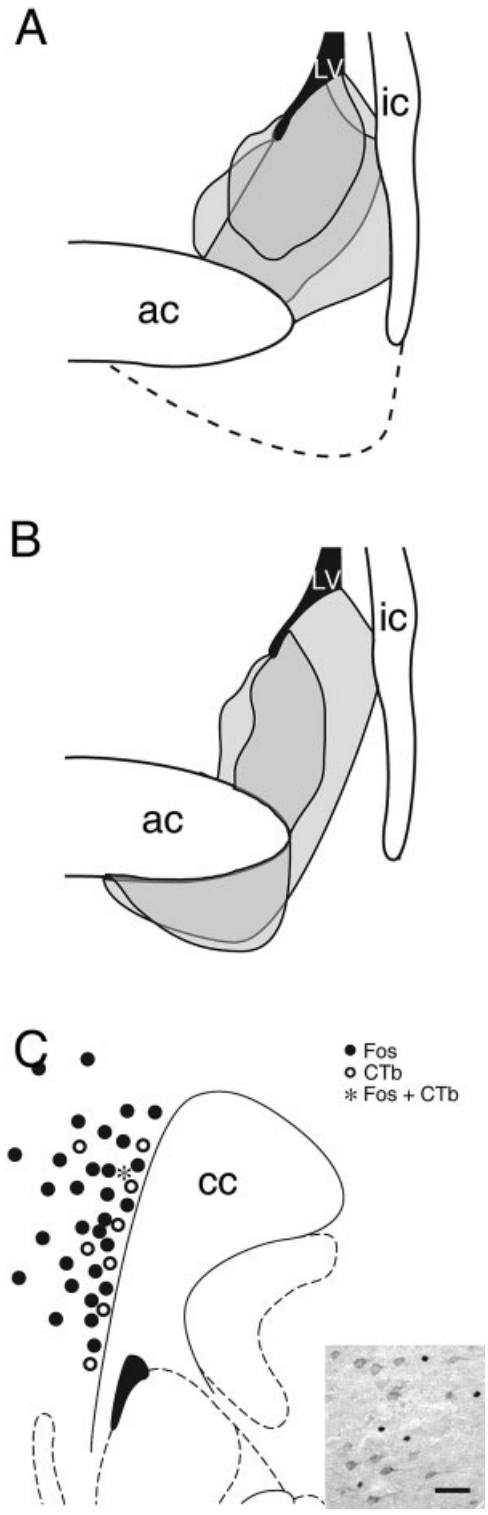

Fig. 8. Localization of retrograde tracer and Fos protein in mPFC cells of animals that had received BNST CTb deposits. **A:** A schematic representation of the successful dorsal and ventral BNST CTb deposit sites adapted from camera lucida drawings. **B:** A schematic representation of the successful dBNST CTb deposit sites adapted from camera lucida drawings. **C:** A schematic coronal diagram illustrating the distribution of Fos-IR (filled circle), CTb-IR (open circle), and double-labeled (star) neurons in the mPFC ipsilateral to the vBNST CTb deposit in an animal subjected to air puff. One symbol corresponds to ten cells. Inset: A photomicrograph of a Fos-IR and CTb-IR cells seen in the ipsilateral mPFC after a CTb deposit in the vBNST and air puff. ac, anterior commissure; cc, corpus callosum; CTb, cholera toxin b subunit; ic, internal capsule; LV, lateral ventricle. Scale bar = 100 μm in A; 200 μm in B; 50 μm in the inset.

lease with a mPFC lesion, but this was not statistically significant. The discrepancy between the present study and those conducted previously cannot be easily explained. It is possible that strain differences in the animals used may explain the apparent differences. Rats of different strains have been clearly shown to display different behavioral, endocrine, and neuronal responses to stress (Woolfolk and Holtzman, 1995; Rittenhouse et al., 2002; Ma and Morilak, 2004). Differences in the type of stressor used could also account for this discrepancy, restraint being the stressor used in both Diorio (1993) and Figueiredo's (2003) studies.

Role of the BNST in the mpPVN CRF cell response to air puff

The results of the present study identified the vBNST as the only candidate relay population examined that displayed significantly altered responsiveness to the psychological stressor air puff after a lesion to the mPFC. There is much evidence to indicate that the BNST does play an important role in the mPFC-modulated response to stress. The vBNST has previously been shown both to receive direct projections from the mPFC and to project, in turn, to the mpPVN (e.g., Hurley et al., 1991; Sawchenko et al., 2000). There is also a large body of functional evidence to suggest a role for the vBNST in regulation of the response to stress, and, as is the case with the mPFC, the role of the BNST in moderating stress responses seems to be dependent on the stressor. There is evidence from BNST-lesion studies that the influence of the BNST is important to the HPA axis response to a physical stressor (Crane et al., 2003a) and to a conditioned stressor (Gray et al., 1993). However, the same effects of a BNST-lesion have not, until now, been demonstrated with an acute psychological stressor (Gray et al., 1993; Crane et al., 2003a). The response of the BNST to a psychological and a physical stressor has, however, been shown to be affected by a lesion of the mPFC (Figueiredo et al., 2003), implying a role for the BNST in the response to both types of stress.

In addition to a role in activation of the mpPVN, the BNST also clearly influences many other stress-sensitive brain regions, as indicated by a comprehensive decrease in extra-hypothalamic Fos expression in response to air puff in the BNST-lesioned animals of this study. Interestingly, the BNST-lesioned animals also showed a decrease in mPFC neuronal activation with air puff. This may imply a direct communication between the BNST and mPFC, but the effects of the BNST-lesions were so global as to preclude any conclusions on direct relationships based on these results alone. It is unfortunate that in this investigation BNST lesions could not be confined to the ventral region of this nucleus and thereby directly test the role of this subregion in the mpPVN stress response. However, it has been found to be very difficult to achieve lesions that encompass the ventral region without affecting the dBNST (Crane et al., 2003a), and so in this investigation the effects of lesions of the whole BNST were examined.

Of course, we cannot exclude the possibility of brain regions additional to the vBNST being involved in modulation of the mpPVN. Indeed, a previous investigation (Figueiredo et al., 2003) identified additional brain regions, such as the MeA, that were affected by a lesion to the mPFC. The present study differs from that of Figueiredo et al. (2003) primarily in that the latter employed in situ hybridization to determine *c-fos* mRNA levels. In addition, Sprague-Dawley rats were used in their study, and it has been demonstrated that this strain of rat shows a particularly prominent MeA Fos response to psychological stress compared with other rat strains (Ma and Morilak, 2004). Nonetheless, this study demonstrates that brain regions additional to the BNST are very likely to also be involved in mPFC modulation of the responses to stress. For example, a substantial population of mpPVN-projecting GABAergic interneurons exists in the peri-PVN region, and this population does receive direct projections from the mPFC (Herman et al., 2002). This network is therefore another potential pathway by which the mPFC may communicate with the mpPVN CRF cells. It should also be noted that the absence of Fos expression in a brain region cannot necessarily be taken as evidence of the absence of a response (Kovacs, 1998).

The effects of BNST lesions on the mpPVN CRF cells could potentially involve both an indirect pathway, such as via brainstem catecholamine cell groups, and a direct pathway. Our experiment combining retrograde tracing with Fos expression is the first to demonstrate that some PVN-projecting vBNST cells respond to a psychological stressor (i.e., air puff). Given evidence that the vBNST contains glutamatergic PVN-projecting cells (Csaki et al., 2000), this suggests that vBNST neurons could directly stimulate the PVN in response to a psychological stressor.

mPFC inputs to the BNST

Deposits of CTb into the BNST in the present study revealed a substantial direct projection from the deeper layers of the mPFC to the ipsilateral vBNST (but not to the dBNST), providing a possible pathway by which the mPFC could influence the response of the mpPVN to psychological stress via the BNST. However, the BNST tracer failed to retrogradely label any mPFC cells that were also activated by air puff. This finding would therefore seem to argue that the response of the BNST to air puff stress is not directly influenced by the mPFC. However, we suggest that vBNST-projecting mPFC cells are controlled by the local GABAergic inhibitory network present in the mPFC (Steketee, 2003). Alternatively, a glutamatergic output to another as-yet-unidentified brain region could also influence the vBNST in response to air puff. This influence of the mPFC would lead to a downregulation of BNST activation with air puff and this pathway would lead, in turn, to a downregulation of mpPVN CRF cell activation via a direct projection from the BNST (Fig. 9). There was no substantial recruitment by air puff of any other brain region retrogradely labeled from the BNST that could serve as an intermediary. However, it is unlikely that the BNST is the only brain region by which the mPFC can communicate with the mpPVN.

CONCLUSION

The findings seen in this study of increased mpPVN CRF and vBNST cell recruitment with a psychological stressor in mPFC-lesioned animals and a reduction in the mpPVN CRF cell response to air puff in BNST-lesioned animals demonstrates the importance of both the mPFC and the vBNST in response to this stressor. We also sug-

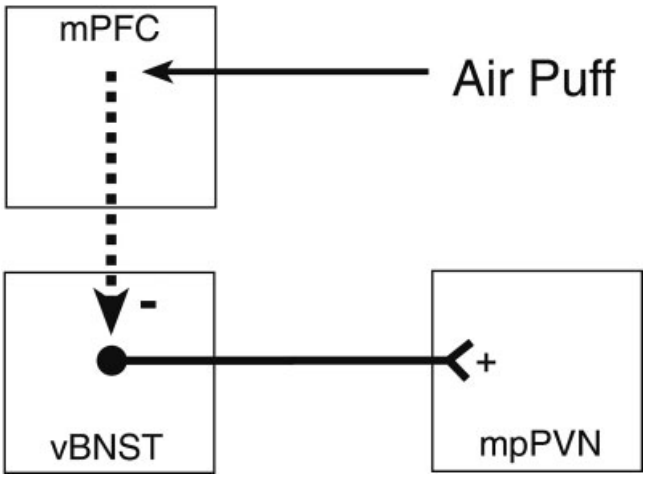

Fig. 9. A schematic diagram summarizing the hypothesized pathway by which the mPFC modulates mpPVN CRF cell responses to stress. It is suggested that air puff activates the mPFC, which then inhibits, via a polysynaptic pathway, the direct excitatory output of the vBNST to the mpPVN. The net result is an inhibition of mpPVN CRF cell activation seen in response to air puff. mPFC, medial prefrontal cortex; mpPVN, medial parvocellular region of the paraventricular hypothalamic nucleus; vBNST, ventral bed nucleus of the stria terminalis.

gest here that the mPFC may suppress the mpPVN CRF cell response to stress via a pathway involving the BNST. Thus, the effects of the mPFC on mpPVN CRF cell stress responses may occur, at least partially, via a direct connection between the vBNST and PVN in response to indirect input from the mPFC.

LITERATURE CITED

Abraham IM, Kovacs KJ. 2000. Postnatal handling alters the activation of stress-related neuronal circuitries. Eur J Neurosci 12:3003–3014.

Black PH. 1994. Central nervous system-immune system interactions: psychoneuroendocrinology of stress and its immune consequences. Antimicrob Agents Chemother 38:1–6.

Bornstein SR, Chrousos GP. 1999. Adrenocorticotropin (ACTH)- and non-ACTH-mediated regulation of the adrenal cortex: neural and immune inputs. J Clin Endocrinol Metab 84:1729–1736.

Brake WG, Flores G, Francis D, Meaney MJ, Srivastava LK, Gratton A. 2000. Enhanced nucleus accumbens dopamine and plasma corticosterone stress responses in adult rats with neonatal excitotoxic lesions to the medial prefrontal cortex. Neuroscience 96:687–695.

Buller KM, Smith DW, Day TA. 1999. Differential recruitment of hypothalamic neuroendocrine and ventrolateral medulla catecholamine cells by non-hypotensive and hypotensive hemorrhages. Brain Res 834:42–54.

Buller KM, Dayas CV, Day TA. 2003. Descending pathways from the paraventricular nucleus contribute to the recruitment of brainstem nuclei following a systemic immune challenge. Neuroscience 118:189–203.

Crane JW, Buller KM, Day TA. 2003a. Evidence that the bed nucleus of the stria terminalis contributes to the modulation of hypophysiotropic corticotropin-releasing factor cell responses to systemic interleukin-1beta. J Comp Neurol 467:232–242.

Crane JW, Ebner K, Day TA. 2003b. Medial prefrontal cortex suppression of the hypothalamic-pituitary-adrenal axis response to a physical stressor, systemic delivery of interleukin-1beta. Eur J Neurosci 17:1473–1481.

Csaki A, Kocsis K, Halasz B, Kiss J. 2000. Localization of glutamatergic/aspartatergic neurons projecting to the hypothalamic paraventricular nucleus studied by retrograde transport of [3H]D-aspartate autoradiography. Neuroscience 101:637–655.

Dayas CV, Buller KM, Crane JW, Xu Y, Day TA. 2001. Stressor categorization: acute physical and psychological stressors elicit distinctive recruitment patterns in the amygdala and in medullary noradrenergic cell groups. Eur J Neurosci 14:1143–1152.

Diorio D, Viau V, Meaney MJ. 1993. The role of the medial prefrontal cortex (cingulate gyrus) in the regulation of hypothalamic-pituitary-adrenal responses to stress. J Neurosci 13:3839–3847.

Duncan GE, Knapp DJ, Breese GR. 1996. Neuroanatomical characterization of Fos induction in rat behavioral models of anxiety. Brain Res 713:79–91.

Ehrhart-Bornstein M, Hinson JP, Bornstein SR, Scherbaum WA, Vinson GP. 1998. Intraadrenal interactions in the regulation of adrenocortical steroidogenesis. Endocr Rev 19:101–143.

Espejo EF, Minano FJ. 1999. Prefrontocortical dopamine depletion induces antidepressant-like effects in rats and alters the profile of desipramine during Porsolt's test. Neuroscience 88:609–615.

Figueiredo HF, Bruestle A, Bodie B, Dolgas CM, Herman JP. 2003. The medial prefrontal cortex differentially regulates stress-induced c-fos expression in the forebrain depending on type of stressor. Eur J Neurosci 18:2357–2364.

Floyd NS, Price JL, Ferry AT, Keay KA, Bandler R. 2001. Orbitomedial prefrontal cortical projections to hypothalamus in the rat. J Comp Neurol 432:307–328.

Gray TS, Piechowski RA, Yracheta JM, Rittenhouse PA, Bethea CL, Van de Kar LD. 1993. Ibotenic acid lesions in the bed nucleus of the stria terminalis attenuate conditioned stress-induced increases in prolactin, ACTH and corticosterone. Neuroendocrinology 57:517–524.

Herman JP, Cullinan WE. 1997. Neurocircuitry of stress: central control of the hypothalamo-pituitary-adrenocortical axis. Trends Neurosci 20:78–84.

Herman JP, Cullinan WE, Watson SJ. 1994. Involvement of the bed nucleus of the stria terminalis in tonic regulation of paraventricular hypothalamic CRH and AVP mRNA expression. J Neuroendocrinol 6:433–442.

Herman JP, Tasker JG, Ziegler DA, Cullinan WE. 2002. Local circuit regulation of paraventricular nucleus stress integration glutamate — GABA connections. Pharmacol Biochem Behav 71:457–468.

Hurley KM, Herbert H, Moga MM, Saper CB. 1991. Efferent projections of the infralimbic cortex of the rat. J Comp Neurol 308:249–276.

Ju G, Swanson LW. 1989. Studies on the cellular architecture of the bed nucleus of the stria terminalis in the rat. I. Cytoarchitecture. J Comp Neurol 280:587–602.

Kovacs KJ. 1998. c-Fos as a transcription factor: a stressful (re)view from a functional map. Neurochem Int 33:287–297.

Lacroix L, Spinelli S, White W, Feldon J. 2000. The effects of ibotenic acid lesions of the medial and lateral prefrontal cortex on latent inhibition, prepulse inhibition and amphetamine-induced hyperlocomotion. Neuroscience 97:459–468.

Ma S, Morilak DA. 2004. Induction of FOS expression by acute immobilization stress is reduced in locus coeruleus and medial amygdala of Wistar-Kyoto rats compared to Sprague-Dawley rats. Neuroscience 124:963–972.

Moga MM, Saper CB, Gray TS. 1989. Bed nucleus of the stria terminalis: cytoarchitecture, immunohistochemistry, and projection to the parabrachial nucleus in the rat. J Comp Neurol 283:315–332.

Palmer AA, Printz MP. 1999. Strain differences in Fos expression following airpuff startle in Spontaneously Hypertensive and Wistar Kyoto rats. Neuroscience 89:965–978.

Pignatelli D, Magalhaes MM, Magalhaes MC. 1998. Direct effects of stress on adrenocortical function. Horm Metab Res 30:464–474.

Rittenhouse PA, Lopez-Rubalcava C, Stanwood GD, Lucki I. 2002. Amplified behavioral and endocrine responses to forced swim stress in the Wistar-Kyoto rat. Psychoneuroendocrinology 27:303–318.

Sawchenko PE, Brown ER, Chan RK, Ericsson A, Li HY, Roland BL, Kovacs KJ. 1996. The paraventricular nucleus of the hypothalamus and the functional neuroanatomy of visceromotor responses to stress. Prog Brain Res 107:201–222.

Sawchenko PE, Li HY, Ericsson A. 2000. Circuits and mechanisms governing hypothalamic responses to stress: a tale of two paradigms. Prog Brain Res 122:61–78.

Smith DW, Day TA. 1993. Neurochemical identification of fos-positive neurons using two-colour immunoperoxidase staining. J Neurosci Methods 47:73–83.

Smith DW, Buller KM, Day TA. 1995. Role of ventrolateral medulla cate-

cholamine cells in hypothalamic neuroendocrine cell responses to systemic hypoxia. J Neurosci 15:7979–7988.

Spencer SJ, Fox JC, Day TA. 2004. Thalamic paraventricular nucleus lesions facilitate central amygdala neuronal responses to acute psychological stress. Brain Res 997:234–237.

Steketee JD. 2003. Neurotransmitter systems of the medial prefrontal cortex: potential role in sensitization to psychostimulants. Brain Res Brain Res Rev 41:203–228.

Sullivan RM, Gratton A. 1999. Lateralized effects of medial prefrontal cortex lesions on neuroendocrine and autonomic stress responses in rats. J Neurosci 19:2834–2840.

Tache Y, Monnikes H, Bonaz B, Rivier J. 1993. Role of CRF in stress-related alterations of gastric and colonic motor function. Ann N Y Acad Sci 697:233–243.

Thrivikraman KV, Nemeroff CB, Plotsky PM. 2000. Sensitivity to glucocorticoid-mediated fast-feedback regulation of the hypothalamic-pituitary-adrenal axis is dependent upon stressor specific neurocircuitry. Brain Res 870:87–101.

van Eden CG, Buijs RM. 2000. Functional neuroanatomy of the prefrontal cortex: autonomic interactions. Prog Brain Res 126:49–62.

Verberne AJ, Owens NC. 1998. Cortical modulation of the cardiovascular system. Prog Neurobiol 54:149–168.

Watanabe T, Morimoto A, Morimoto K, Nakamori T, Murakami N. 1991. ACTH release induced in rats by noradrenaline is mediated by prostaglandin E2. J Physiol 443:431–439.

Whitnall MH. 1993. Regulation of the hypothalamic corticotropin-releasing hormone neurosecretory system. Prog Neurobiol 40:573–629.

Woolfolk DR, Holtzman SG. 1995. Rat strain differences in the potentiation of morphine-induced analgesia by stress. Pharmacol Biochem Behav 51:699–703.